Four Elements Reconfigurable MIMO Antenna for Dual Band Applications

Vipin Choudhary[1], Manoj Kumar Meshram[1*], and Jan Hesselbarth[2]

[1]Department of Electronics Engineering, Indian Institute of Technology (BHU), Varanasi 221005, India
[2] Institute for High Frequency, Stuttgart University, Stuttgart, Germany
[*]mkmeshram.ece@iitbhu.ac.in

Abstract. Four-element reconfigurable multiple-input-multiple-output (MIMO) antennas for dual band applications are proposed. The frequency reconfigurability of the proposed antennas is achieved by incorporation of three PIN diodes within the single element. The antenna covers multiple switchable operating bands for Worldwide Interoperability for Microwave Access (Wi-MAX)/Wireless Local Area Network (WLAN) applications (3.4-3.6GHz, 3.8-3.86GHz, 5.18-5.27GHz, 5.35-5.5GHz and 5.67-5.8GHz). The proposed MIMO antenna consists of 2x2 elements on a single FR4 substrate. The combinations of MIMO and reconfigurable antenna provide improved performance in terms of envelope correlation coefficient (ECC) and channel capacity loss (CCL) in multiple-frequency bands. The MIMO antenna system performance including the isolation, ECC, CCL, and the diversity gain (DG) are simulated and measured. High isolation (≥ 25dB) is achieved between reconfigurable MIMO antenna ports without any internal and external decoupling network. The proposed antenna has sufficient performance that makes it suitable for indoor access points (IAPs).

Keywords: Reconfigurable Antennas, MIMO Antennas, Reconfigurable MIMO Antennas

1. Introduction

Modern wireless system implements multiple-input multiple-output (MIMO) technology using multi-antennas to fulfil increasing demands of higher data transmission rate, good reliability and better communication quality which lead to increase the transmission speed and more capacity of the wireless system without overburden on transmission power.

In wireless systems, multiple antennas (MIMO antenna) are used in wireless local area networks (WLANs) to improve the overall channel capacity and to overcome the multipath fading problem results better communication system [1-3]. However, for the efficient use of available RF-spectrum, multiple services and encroachment on number of users placing separate antennas for different applications in portable or small devices (like cell phones, user access points, etc.) increases design challenges and costs [4]. Thus, to overcome multipath fading and resourcefully use of RF-spectrum the reconfigurable technologies are merged with MIMO technologies named as reconfigurable MIMO. Various antennas have been reported with omni-directional patterns for indoor and outdoor wireless access points (WAPs), because the pattern diversity of these antennas allow a good communication link in between transmitter and receiver [5-12].

The most commonly used antennas for WAPs are microstrip patch antennas. Various reconfigurable antennas and multi-element MIMO antennas are studied [7-12] for Wi-MAX and WLAN application using different methodologies. The envelope correlation coefficient (ECC) and diversity gain performance parameters of Wi-MAX and 802.11 WLAN have been calculated using mathematical equations based on other important parameters.

One of essential factor that determines the performance of the MIMO antenna systems is the isolation between the antenna input ports. To ameliorate the MIMO antenna performance, several internal and external decoupling networks, techniques and methods have been reported to increase the isolation between the MIMO antenna system such as defective ground structure (DGS), electromagnetic band gap (EBG), neutralization line, introducing air gap, etc. [13-18]. In [14], two parallel planar inverted-F antennas with DGS have been used to achieve good isolation but for large scale structure experienced decrement in front to back radiation ratio. In another approaches, neutralization line [15, 16] and EBG [17, 18] were introduced but found that the design challenges were increased for reducing mutual coupling using these techniques.

As compared to traditional multiple antennas, reconfigurable MIMO antennas provide many advantages such as compact size and better gain on desired bandwidth.

The basic principle of reconfigurable antenna is changing/blocking the current density in an element by electrical or mechanical switches. Electrical switches such as PIN diodes, varactor diodes, MEMS switches [19-23] are used. In recent years, lots of studies on frequency reconfigurable antennas have been carried out using PIN diodes in [19-21].

Generally, large numbers of switches (like varactors, PIN diodes, etc.) were used in single element that would lead to involve more DC-bias circuits and increase design complexity. In proposed reconfigurable MIMO antennas, the number of switching components are reduces up to three per element which covers three different frequency bands.

In this paper, a compact frequency reconfigurable MIMO antenna using active and passive components (i.e. inductors, capacitors and PIN diodes) is presented. High isolation (≥25dB) is achieved without any internal and external decoupling network. It is due to physical separation between the MIMO antenna elements. Thus, the design challenges and cost are reduced significantly.

The proposed reconfigurable MIMO antenna likely to operate in different switchable frequency bands (Wi-MAX/WLAN), makes the antenna dynamic according to usability and robust to environmental scenarios (multipath,

DOI: http://dx.doi.org/10.32452/IJAMT.2022.274282

fading effect etc.). Figure 1 shows the block diagram of proposed four element reconfigurable MIMO antenna accompanied by matching network, isolation, switching network and external DC-bias circuit.

2. Antenna design and configuration

The configuration of single element is illustrated in Fig. 2. The presented antenna is designed and fabricated on FR4 substrate which has a dielectric constant (ε_r) = 4.4, loss tangent (tanδ) = 0.02 and thickness (h) = 1.6mm. The simulation and optimization of antenna design is carried out using ANSYS High-Frequency Structure Simulator (HFSS) software [24]. The optimized shape parameters of the proposed MIMO antennas are shown in Table 1.

2.1. Equivalent circuit model of PIN diode

One of the most commonly operated switching components is RF PIN diodes. In this paper, RF PIN diodes are used as the switching elements to accomplish the frequency reconfiguration in the proposed reconfigurable-MIMO antenna design.

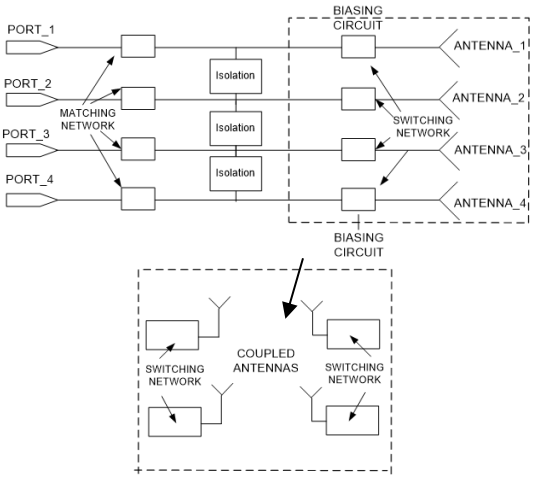

Fig. 1. Block diagram of four element reconfigurable MIMO antenna with switching network.

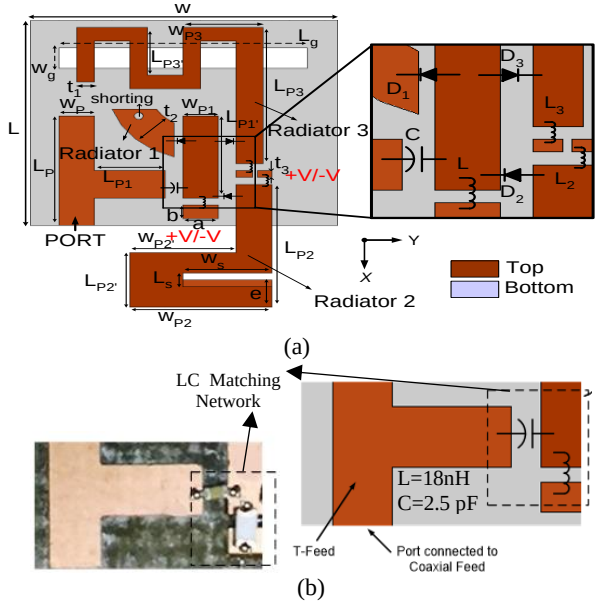

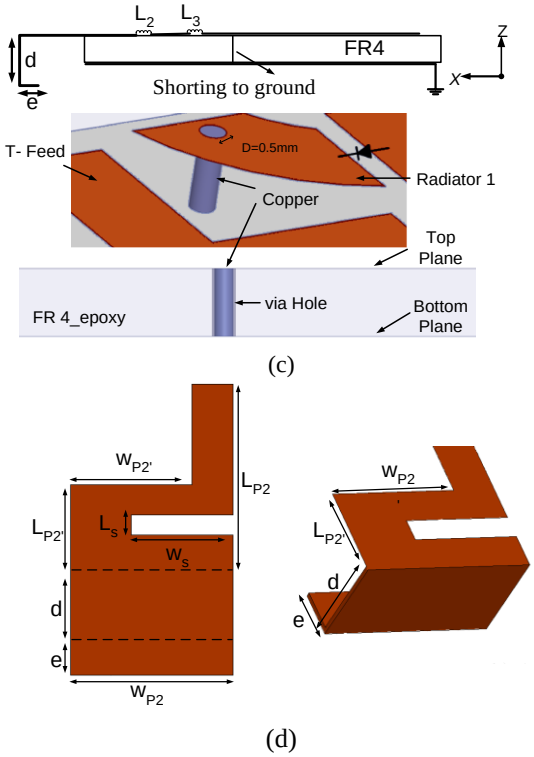

Fig. 2. Reconfigurable antenna: (a) Single-element of the proposed antenna, (b) LC matching network, (c) Side view, (d) Unfolded and folded view of Radiator 2.

Table 1 Design parameters (unit: mm)

Para.	Values	Para.	Values	Para.	Values
L	15	L_{P2}'	4	W_{P3}	4.5
W	18	W_{P2}	8	W_g	1.5
L_P	8	W_{P2}'	6	L_g	14
W_P	2	L_S	1	a	2
L_{P1}	4	W_S	5	b	1
W_{P1}	2	L_{P3}	10	d	4
L_{P2}	9	L_{P3}'	3.5	e	2

The RF PIN diodes models are chosen as Skyworks-SMP1345 [12]. The equivalent circuit models of the diodes for ON/OFF or 1/0 states are shown in Fig.3.

It consists of a series inductance (*L*1) and a low resistance (*R*1) when the PIN-diode is in ON state, while a series inductance (L1) and a parallel combination of a resistance (*R*2) and capacitance (C1) when the PIN-diode is in OFF state. The values for the ON state: L1 = 0.7nH and R1 = 1.5Ω, and the OFF state: L1 = 0.7nH, R2 = 2MΩ and C1 = 0.15pF are chosen for simulation [12]. The proposed antenna is constructed based on matching network and equivalent circuit modeling of PIN diode as a switching network model. The models are applied to simulate, design and optimize the antenna parameters.

2.2. Single-element reconfigurable antenna

Each element of reconfigurable MIMO antenna consists of three asymmetric radiators, which are connected to a common T-shaped microstrip feed line as shown in Figure 2. Since, the number of radiators attached to single feed line will cause

DOI: http://dx.doi.org/10.32452/IJAMT.2022.274282

impedance mismatching. Therefore, an LC-matching network is placed to provide impedance matching in between the feed line and the radiators. The value of capacitance C = 2.5pF and inductance L =18nH are optimized manually. It can also be obtained by using ADS software.

The individual element of proposed antenna is comprises of three different shaped radiator. So, each radiator is designed and implemented different techniques (such as shorting to ground, defective ground structure-DGS and notch on patch) to cover multiple switchable operating bands. The multiband reconfigurable antenna is realized by merging three RF PIN-diodes to three different shaped patch antennas and using external DC-biasing circuit. Diodes are designated as Diode 1-3(D_1, D_2, and D_3).

2.3. Parametric study

To determine the *S*-parameter bandwidth at different resonant bands of the single element reconfigurable MIMO antenna, parametric study is performed. To perform the parametric study the shape and size of the board is chosen same as the optimized structure. For the initial optimization, at a time single diode is ON and rest of the diodes are kept in OFF state are considered.

Figure 4 shows the *S*-parameters of single reconfigurable MIMO element with different configuration of RF PIN diodes. D1-ON represents Diode 1 is in 'ON' state and Diode 2-3 are in 'OFF' state. Similarly, D2-ON and D3-ON represents Diode 2 and Diode 3 is ON, respectively and other diodes are in OFF state. It is observed that when Diode 1 or Diode 3 is in ON state various tunable WLAN frequency bands between 5.1 GHz to 5.8 GHz are achieved and if Diode 2 is in ON state it covers Wi-MAX frequency bands. The basic switching mechanism of frequency reconfiguration is that the effective length (L_{eff}) of the radiators and path of antenna current distribution are changed to achieve approximately 2 GHz of shift in the frequency band.

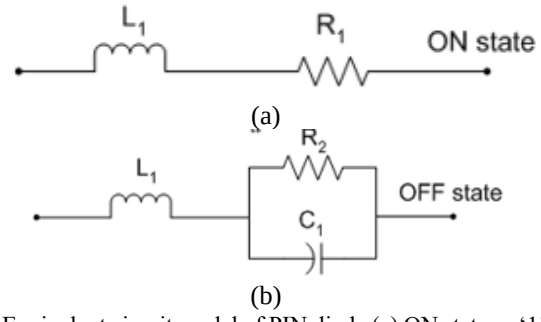

Fig. 3. Equivalent circuit model of PIN diode (a) ON state or '1' state, (b) OFF state or '0' state.

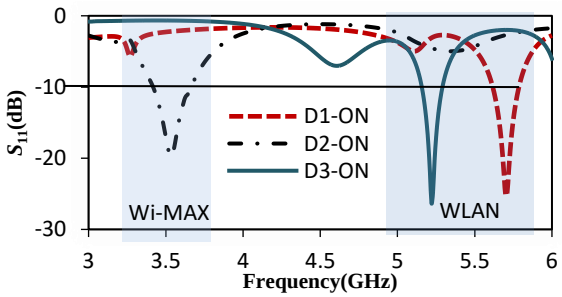

Fig. 4. S-parameters of single element using PIN-diodes as a switch at different diode configuration.

The proposed geometrical parameters examined for study are the placement of shorting position to ground "A", "B", "C" of radiator 1 (see Figure 5a), the slot length "Ws", folded length "d" and "e" of radiator 2 (see Figure 2(d)), the DGS length "Lg" and width "Wg" of radiator 3. The resonant frequencies are tuned by analyzing particular geometrical parameter meanwhile the other parameters are kept constant.

Figure 5(a) shows the variation of reflection coefficient of the antenna with frequency by considering the shorting position to ground as parameter. It can be seen that the position A (shorting to ground) provides sharper peak at upper frequencies than that of the position B and C. This is mainly because of the quarter-wavelength shorted strip ($\lambda_g/4$ @ 5.65GHz) from point A to T-feed line. As can be seen in Figure 2 (d) that the length of radiator 2 (L_{p2}+d+e) is less than half-wavelength ($\lambda_g/2$ @ 3.6GHz). Further, to increase the electrical length of radiator 2 a slot (Ls x Ws) is introduced which gives minimum reflection within Wi-MAX band. Further, Figure 5(b)-(d) shows the variation of reflection coefficient with frequency for slot parameter "Ws", "d", and "e" of radiator 2. It is observed from Figure 5(b) that the increase in the slot width "W_s" results the shift in resonant frequency band towards lower frequency and a sharper roll-off at the Wi-MAX (3.3-3.8GHz) frequency band while no change is observed in the upper frequency band (5-6GHz). It is due to the increment in the effective length of radiator 2 as expected. Simply the optimized S_{11} result of radiator 2 validated by increase or decrease in slot parameter "d" and "e" leads to mismatch as shown in Figure 5(c) and 5(d), respectively.

Figure 6 shows the variation of the reflection coefficient with frequency for DGS parameters of the radiatior 3 when diode 3 is in the ON state. It is seen from Figure 6(a) and 6(b) that the WLAN frequency band (5.18 GHz – 5.27 GHz) is achieved by incorporating the DGS on the ground plane of radiator 3 with parameter "W_g" and "L_g". When W_g=0 (without DGS) indicates more reflections. Hence, position 'A' as shorting to ground, W_s = 5mm, d = 4mm, e = 2mm L_g= 14mm and W_g = 1.5mm are selected as the optimal values for which good S_{11} (<-10dB) is observed in Wi-MAX and WLAN frequency bands respectively.

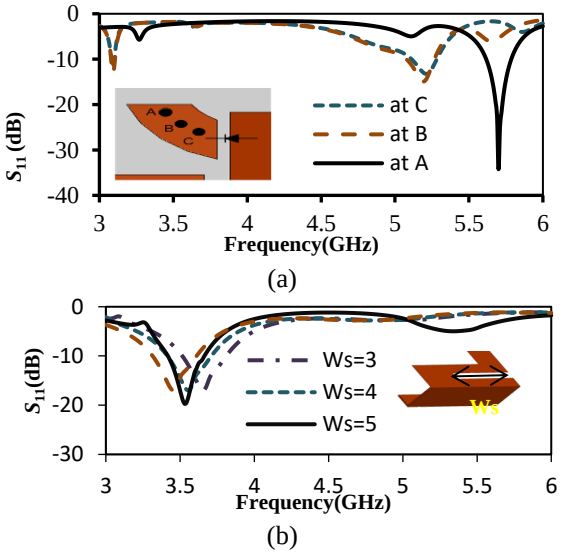

DOI: http://dx.doi.org/10.32452/IJAMT.2022.274282

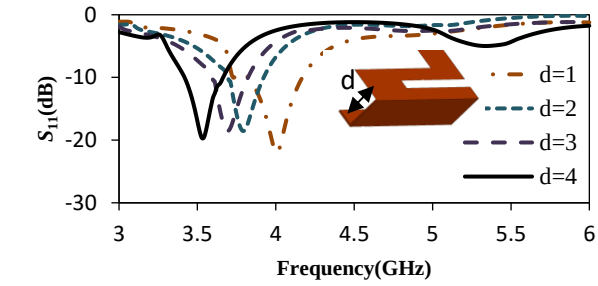

(c)

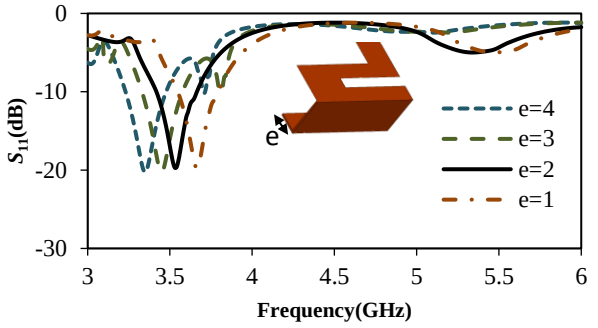

(d)

Fig. 5. Parametric variation of slot parameters of radiator 2 when diode 2 is in ON state; (a) Shorting position on radiator 1, (b) slot parameters Ws , (c) d and, (d) e of radiator 2 (Unit: mm).

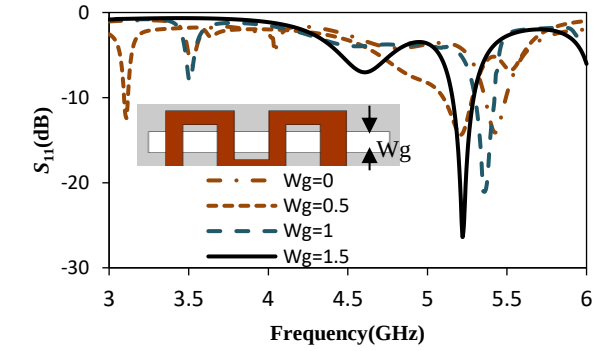

(a)

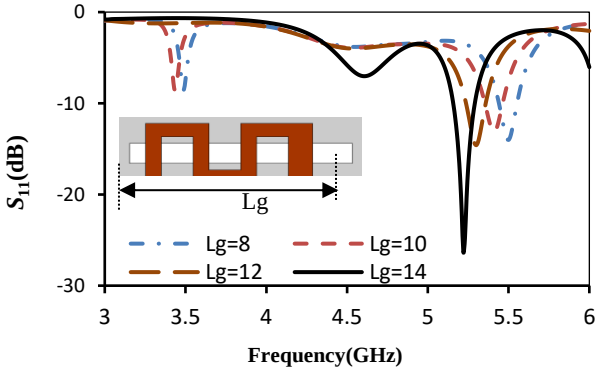

(b)

Fig. 6. Parametric variation of DGS parameters of radiator 3 when Diode 3 is in ON state: (a) Wg (b) Lg. (Unit: mm)

2.4. Four-elements reconfigurable MIMO antenna

The reconfigurable antennas are arranged in such a manner that the radiating patches of all the antennas are on the top and ground structure on bottom of the H-shaped substrate with dimension 60x80mm^2. Figure 7 shows the prototype of proposed four element reconfigurable MIMO antenna. The antennas are named as Antenna1-4. The prototype is fabricated by using T-Tech (quick circuit prototype systems) micro milling machine.

The shape of substrate reduces the size of overall device and also provides space for indicators, display unit and input-output device ports. The proposed structure not only provides the basic need of high isolation (>25dB) over the entire resonant frequency bands, but also utilizes the plane between antenna elements for device components. Since all four elements are identical therefore the reflection *S*-parameter will be remained same for all the elements. Only coupling S-parameters (S_{12}, S_{13}, and S_{14}) will change due to placement of antennas on different locations and different possible combinations of the PIN diodes.

There are three PIN diodes are used with each MIMO element to achieve frequency reconfigurability. Hence, six possible combinations namely S1 to S6 are considered for the present study. Table 2 provides the various switching state of the PIN diode in binary form (0 for OFF and 1 for ON states).

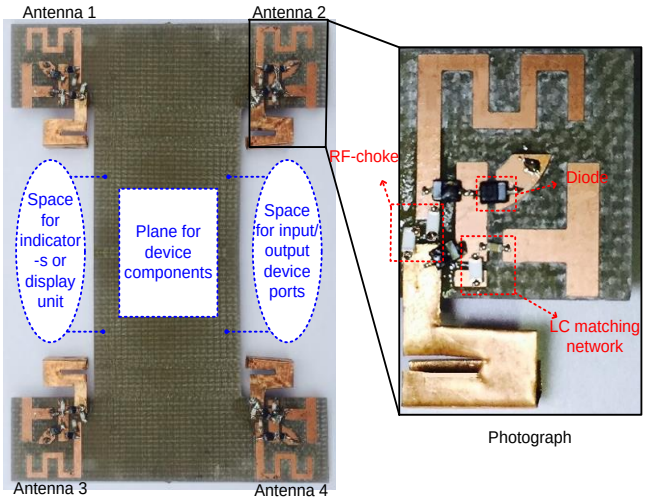

Fig. 7. Prototype of 4-element reconfigurable MIMO antenna.

3. Results and discussion

3.1. S-parameters of the proposed antenna

The measurement is executed on vector network analyzer VNA Master MS2038C (5 kHz-20 GHz). The simulated and measured frequency bands, isolation and simulated radiation efficiency (η_r) for different switching state are presented in Table 2. As expected, the radiation efficiency at the switching states S1, S2, and S3 has higher values as compare to S4, S5, and S6. This is because of more number of ON states of PIN diodes which results in larger ohmic losses and thus reduces the overall radiation efficiency of the antenna. While all the four elements are similar, the reflection *S*-parameters of all the antenna elements are symmetrical for identical switching configuration. The simulated and measured *S*-parameters are plotted in Figure 8.

It is observed that the simulated and measured results of *S*-parameters show good performance with S_{11} (<-10dB) and S_{12} (<-25dB) parameters for the switching states S1 (5.67-5.8GHz), S3 (5.18-5.27GHz), S5 (5.35-5.55GHz) are situated in WLAN

(5-5.9GHz), state S2 (3.4-3.61GHz), S6 (3.8-3.86GHz) are located in Wi-MAX (3.3-3.8GHz) and state S4 (3.37-3.6 GHz and 4.9-5.1GHz) covers both WLAN and Wi-MAX frequency bands. The measured results are in close agreement with the simulated results with little disagreement (see Figure 8). The slight difference mainly attributed due to fabrication tolerances, equivalent circuit models of RF PIN diodes, more soldering to make good connect and testing environment. Since, all the four parameters are identical, therefore, in Figure 8, the simulated results of other decoupling parameters like S_{13} and S_{14} of the proposed MIMO antenna are plotted. The mutual couplings between antenna elements (i.e. S_{12}, S_{13}, S_{14}) for different states (S1, S2, S3, S4, S5 and S6) are less than 25dB is achieved.

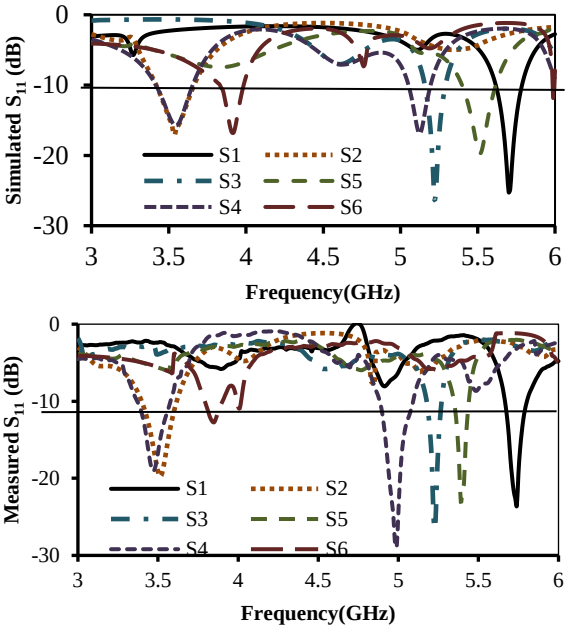

(a)

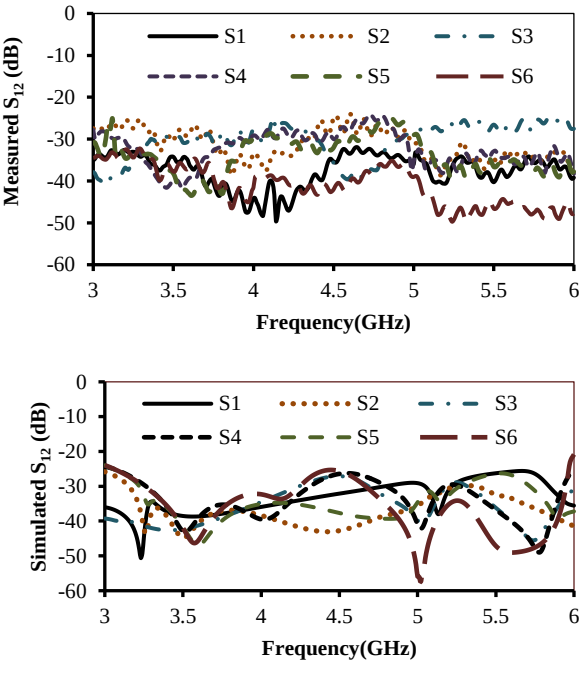

(b)

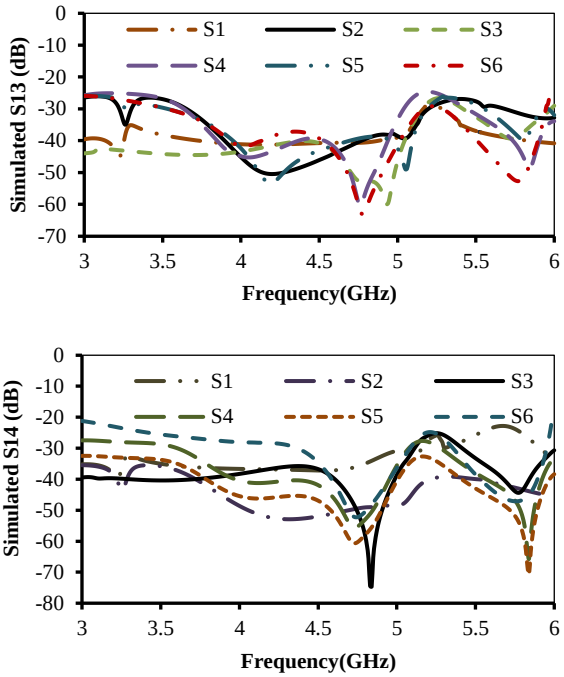

(c)

Fig. 8. S-parameters of the proposed antenna at different states of PIN diodes (a) S_{11}, (b) S_{12}, (c) S_{13} and S_{14}.

3.2. Surface current distribution at different states

The current distribution path on the presented reconfigurable MIMO antenna is responsible for switching different frequency bands. To visualize the basic frequency reconfiguration mechanism, the surface current distribution on the proposed antenna at S1, S2, S3, S4, S5, and S6 states are demonstrated in Figure 9.

It is observed that resonant frequency changes with alter the diodes configuration. It can be clearly observed from Fig 9a-c that when all the ports are excited there is negligible amount of the surface current passes from one antenna port to another antenna port. The spacing between antenna elements cause null in between them.

Further, it can be observed in Figure 9(a) (state S1) and demonstrated by the black arrow, the path length travelled by surface current is smaller which is responsible for upper resonant frequency (5.6GHz). When antenna resonant at lower frequency (3.6GHz), the effective length of element current distribution and effective length of radiator are larger because of PIN diode attach to radiator 2 is in ON state as shown in Fig. 9a (state S2). Furthermore, it can be observed from Figure 9(b) (state S3) that the surface current travels through effective length of radiator expanded over the DGS leads to radiate at upper frequency (5.2GHz). Similarly, nulls are visible in the Figure 9(b) (state S4), 9(c) (state S5) and (state S6) between the antenna elements in different switching states justified the good isolation. However, in the Figure 9(c) (state S6) when all diodes are in ON states (i.e. S6 state) there is very small amount of surface current flow from one antenna element to another antenna element results a little decrement in isolation as seen in Table 2.

DOI: http://dx.doi.org/10.32452/IJAMT.2022.274282

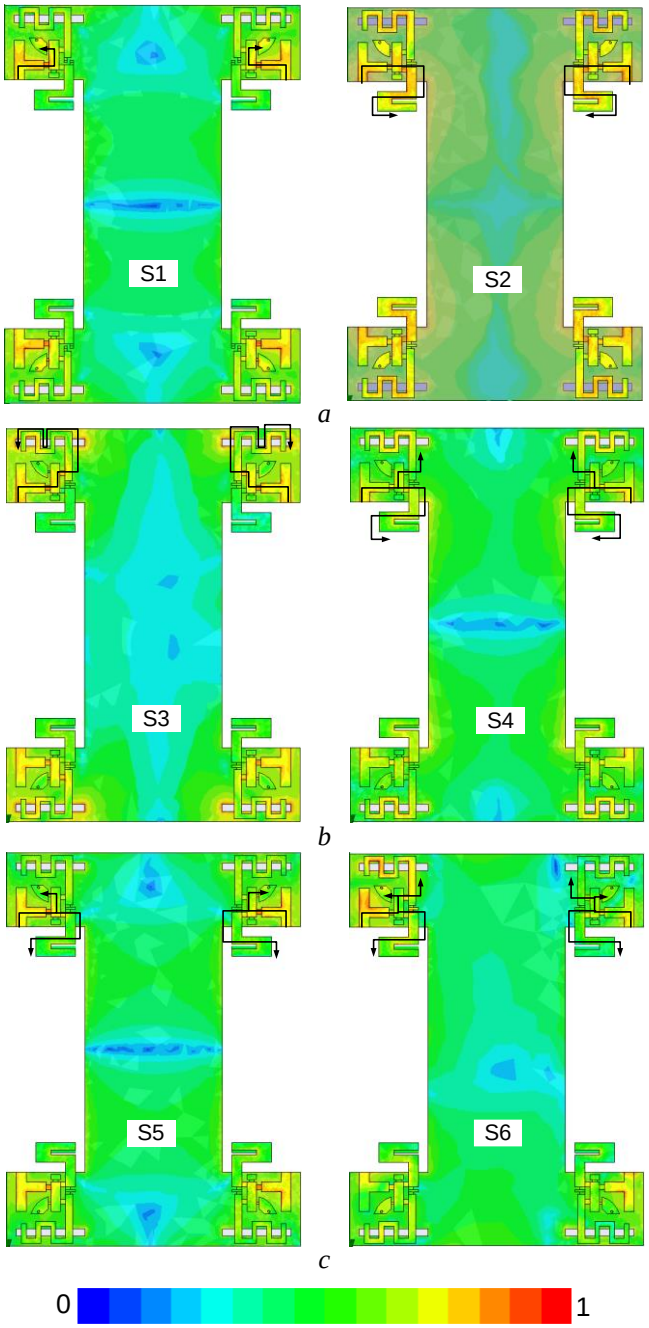

Fig. 9. Current distributions between nearest elements at different switching states, where at S1, S2 state, (b) at S3, S4 state, (c) at S5 and S6 state.

3.3. *Radiation patterns at different states*

The 2D-radation patterns of the proposed antenna in XOZ-plane (E-plane) and YOZ-plane (H-plane) are determined using High-Frequency Structure Simulator software and measured in the anechoic chamber for the different diode configuration at different frequencies. The pyramidal horn antennas (designed for S, C and X-bands) are used as transmitting antenna and the proposed Antenna1 is connected to coaxial detector as receiving antenna located in the far-field region, all the other ports are terminated with 50-ohm matched loads for 2D pattern measurement in XOZ and YOZ-planes. Due to similar behavior of the identical antenna elements, the 2D-radiation pattern of Antenna1 is presented in this article. The simulated and measured results (Normalized gain (dB) versus Angle) in XOZ and YOZ-planes at the six different states are shown in Fig. 10. It can be observed that the corresponding 2D pattern results are almost similar to the each other. However, the fabricating tolerance and the additional parasitic parameters generated by introducing inductor, capacitor and PIN diodes makes experimental radiation patterns slightly differed from the simulated radiation patterns.

Furthermore, it is observed that the pattern appears almost bidirectional and quasi-Omni-directional 2D-radiation patterns in XOZ and YOZ-planes, respectively. The total efficiency of the i^{th} and j^{th} ports is defined as [10].

$$\eta_{total} = \eta_{rad1}(1 - |S_{11}|^2 - |S_{21}|^2) \quad (1)$$

$$\eta_{total} = \eta_{rad2}(1 - |S_{22}|^2 - |S_{12}|^2) \quad (2)$$

where, η_{rad1} and η_{rad2} are the radiation efficiencies when port 1 and port 2 is excited, respectively.

3.4. *MIMO system performance parameters*

The envelope correlation coefficient (ECC) and channel capacity loss (CCL) are the important parameters to analyze the diversity performance of the MIMO antenna. The ECC can be enrolled to determine the degree of similarities between the two or more field patterns. Generally, high envelope correlation means more interference between the two radiation patterns so the acceptable value of this parameter is ECC < 0.5 [3, 10].

The envelope correlation coefficient (ECC) can be evaluated by using eqn (3) and (4) which are discussed in [3, 10-11, 25]. Here, ρ_e represents the envelope correlation coefficient between the i^{th} and j^{th} elements (where $i, j = 1, 2$).

$$\rho_e = \frac{\left|S_{ii}^{*}S_{ij} + S_{ji}^{*}S_{jj}\right|^2}{\left(1-\left|S_{ii}\right|^2-\left|S_{ji}\right|^2\right)\left(1-\left|S_{jj}\right|^2-\left|S_{ji}\right|^2\right)} \quad (3)$$

$$\rho_e = \left|\rho_{ij}\right|^2 = \frac{\left|\iint\left[\vec{F_1}(\theta,\phi)*\vec{F_2}(\theta,\phi)\right]d\Omega\right|^2}{\iint\left|\vec{F_1}(\theta,\phi)\right|^2 d\Omega \iint\left|\vec{F_2}(\theta,\phi)\right|^2 d\Omega} \quad (4)$$

Where, $\vec{F_1}(\theta,\phi)$ and $\vec{F_2}(\theta,\phi)$ represents the beam patterns of the MIMO antenna when port1 and port2 is excited, respectively and $*$ depicts the Hermitian product function. The complex cross-correlation coefficient (ρ) and envelope correlation coefficient (ρ_e) is closely related with $|\rho|^2 \approx \rho_e$. Thus, the relation between diversity gain (G_d) and complex cross-correlation coefficient is [3], [9]

$$G_d = 10 * \sqrt{1-\left|\rho\right|^2} \quad (5)$$

Where, $\sqrt{1-\left|\rho\right|^2}$ term is reducing the diversity gain induced by envelope correlation coefficient. The lower is the value of ECC, the more desirable is the diversity gain.

DOI: http://dx.doi.org/10.32452/IJAMT.2022.274282

Table 2: Diodes configuration and corresponding results

State	D1	D2	D3	Simulated f_L -f_H (GHz)	Measured f_L -f_H (GHz)	Simulated Isolation (dB)	Measured Isolation (dB)	Simulated radiation efficiency (η_r)	Peak gain (dB)
S1	1	0	0	5.61-5.8	5.67-5.8	≥28	>30	70%	5.2
S2	0	1	0	3.4-3.66	3.4-3.61	>35	>38	80%	1.8
S3	0	0	1	5.16-5.2	5.1-5.27	>28	>30	69%	2
S4	0	1	1	3.4-3.65 & 5-5.19	3.37-3.6 & 4.9-5.1	>27	>28	71%	>2.7
S5	1	1	0	5.4-5.61	5.35-5.5	>26	>27	66%	2.5
S6	1	1	1	3.8-3.98	3.8-3.86	≥23	≥22	57%	≥2.5

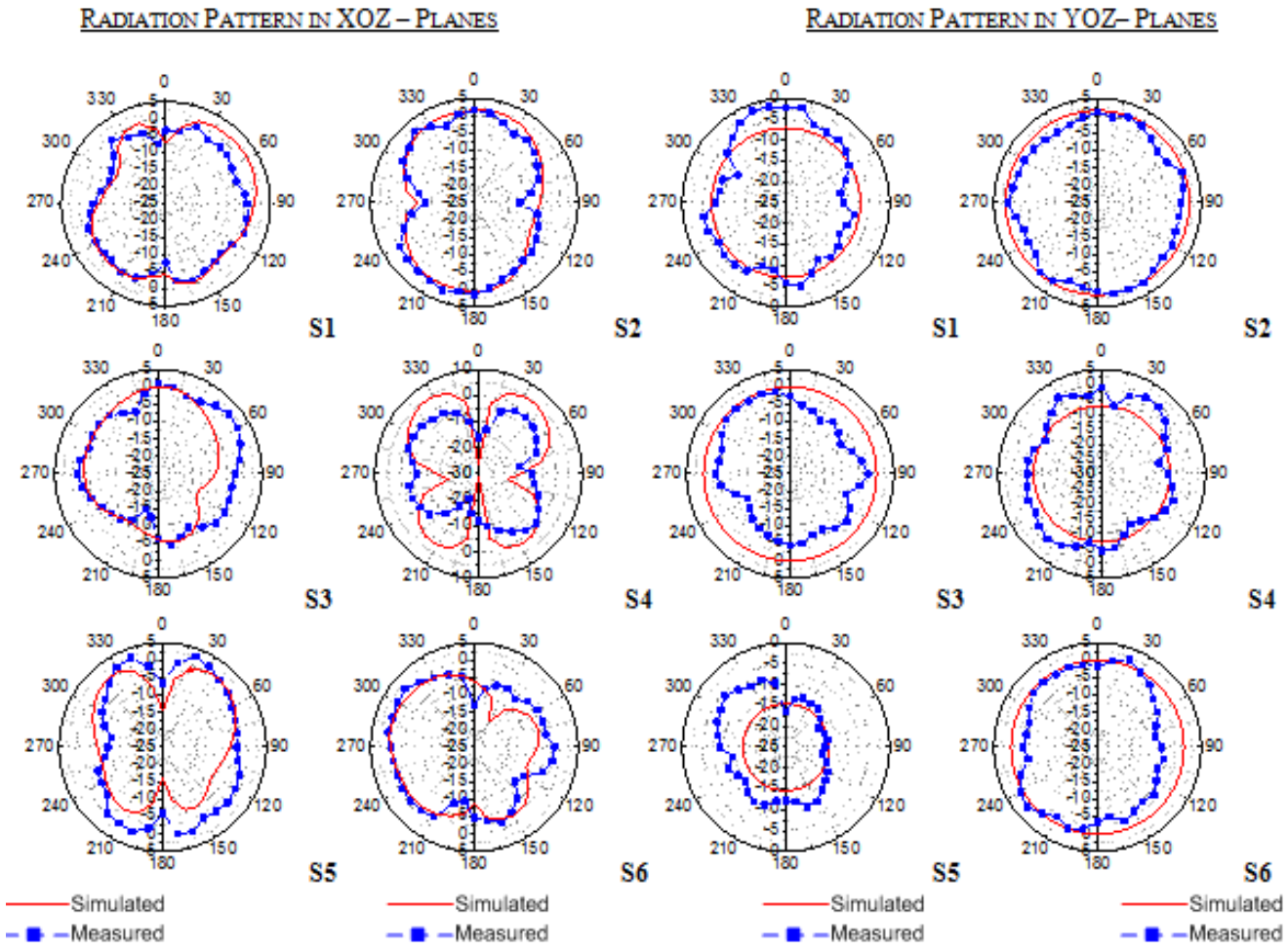

Fig. 10. The simulated and the measured radiation patterns when Port 1 is excited at different states in XOZ-planes and YOZ-planes, respectively (S_1 at 5.8GHz, S_2 at 3.6GHz, S_3 at 5.2GHz, S_4 at 5GHz, S_5 at 5.5GHz and S_6 at 3.8GHz).

Another parameter channel capacity loss (CCL) employed to characterize quality of a multiple antenna system. Thus, the CCL is also computed from the *S*-parameter-based formula [10, 26] as follows:

$$C_{loss} = -\log_2 |\Psi_R| \quad (6)$$

Where, Ψ_R is the receiving antenna correlation matrix.

The matrix elements ρ_{ij} stands the correlation coefficients. The expression shows MIMO system performance and C_{loss} affects by the reflections at the antenna ports.

$$\Psi_R = \begin{pmatrix} \rho_{11} & \rho_{12} \\ \rho_{21} & \rho_{22} \end{pmatrix},$$

Here,

$$\rho_{ii} = 1 - |S_{ii}|^2 - |S_{ij}|^2$$

$$\rho_{ij} = S_{ii}^{*} S_{ij} + S_{ji}^{*} S_{jj}$$

DOI: http://dx.doi.org/10.32452/IJAMT.2022.274282

The MIMO system performance parameters are calculated and shown in Table 3. For good MIMO antenna performance, CCL should be less than 0.40 bits/s/Hz. The measured and simulated results of ECC and CCL are calculated by using the reflection coefficients formula (*S*-parameters) and are shown in Figure 11. It is clear that both ECC and CCL exist within the acceptable limits.

Table 3: MIMO system performance parameters.

Port x-y	Frequency (GHz)	CCL (bits/s/Hz)	ECC	G_d
1-2	3.6	0.24	0.006	9.999
	5	0.126	0.005	9.999
	5.8	0.21	0.001	9.999
1-3	3.6	0.22	0.002	9.999
	5	0.25	0.041	9.998
	5.7	0.32	0.078	9.996
1-4	3.6	0.29	0.072	9.997
	5	0.31	0.085	9.995
	5.7	0.34	0.088	9.995

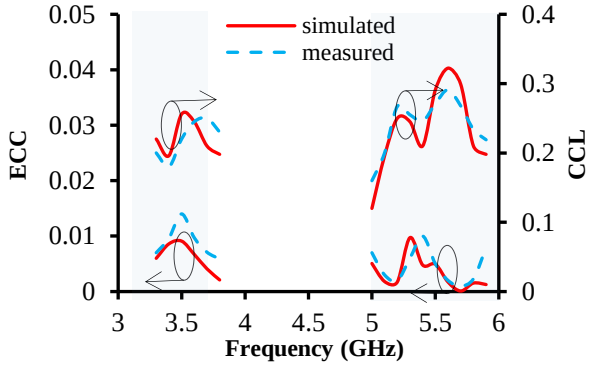

Fig. 11. The simulated and measured ECC and CCL of proposed antenna.

The reconfigurable MIMO antenna is capable of switching (~2GHz bandwidth) and has low CCL (< 0.40 bits/s/Hz) and low ECC (< 0.5) forms a good choice in indoor and outdoor wireless access points (WAPs) for Wi-MAX/m-WLAN applications. The simulated antenna is validated by prototype and tested results.

4. Conclusion

A four-element frequency reconfigurable MIMO antenna is proposed, fabricated and measured. In this work, the antenna designed with omni-directional and bi-directional radiation pattern in *H*- and *E*-planes respectively, for premium WAPs. It has been shown that the multiple bands can be accomplished using three different shaped radiators and equivalent circuit models of RF PIN-diodes as switches. It provides good frequency reconfiguration and high isolation over the operating frequency bands.

References

[1] M.A. Jensen and J.W. Wallace, A review of antennas and propagation for MIMO wireless communications, *IEEE Transactions on Antennas and Propagation*, vol. 52, no.11, pp.2810-2824, 2004.

[2] S.Y. Lin and H.R. Huang, Ultra-wideband MIMO antenna with enhanced isolation, *Microwave and Optical Technology Letters*, vol. 51, no. 2, pp.570-573, 2009.

[3] H.S. Singh, B.R. Meruva, G.K. Pandey, P.K. Bharti, and M.K. Meshram, Low mutual coupling between MIMO antennas by using two folded shorting strips, *Progress In Electromagnetics Research B*, vol. 53, pp.205-221, 2013.

[4] A. Alexiou and M. Haardt, Smart antenna technologies for future wireless systems: trends and challenges, *IEEE communications Magazine*, vol. 42, no. 9, pp.90-97, 2004.

[5] Q. Wu, R. Jin, J. Geng, and M. Ding, Printed omni-directional UWB monopole antenna with very compact size, *IEEE Transactions on Antennas and Propagation*, vol.56, no.3, pp.896-899, 2008.

[6] Y.J. Wu, B.H. Sun, J.F. Li, and Q-J Liu, Triple-band omni-directional antenna for WLAN application, *Progress In Electromagnetics Research*, vol. 76, pp.477-484, 2007.

[7] N. Haider, D. Caratelli, and A.G. Yarovoy, Recent developments in reconfigurable and multiband antenna technology, *International Journal of Antennas and Propagation*, Article ID 869170, 14 pages, 2013.

[8] H.L. Zhu, S.W. Cheung, X.H. Liu, and T.I. Yuk, Design of polarization reconfigurable antenna using metasurface, *IEEE transactions on antennas and propagation*, vol. 62, no.6, pp.2891-2898, 2014.

[9] M. Kelley, C. Koo, H. McQuilken, B. Lawrence, S. Li, A. Han, and G. Huff, Frequency reconfigurable patch antenna using liquid metal as switching mechanism, *Electronics Letters*, vol. 49, no. 22, pp.1370-1371, 2013.

[10] Y.K. Choukiker, S.K. Sharma, and S.K. Behera, Hybrid fractal shape planar monopole antenna covering multiband wireless communications with MIMO implementation for handheld mobile devices, *IEEE Transactions on Antennas and Propagation*, vol. 62, no. 3, pp.1483-1488, 2014.

[11] L. Xiong and P. Gao, Compact dual-band printed diversity antenna for WIMAX/WLAN applications, *Progress In Electromagnetics Research C*, vol. 32, pp.151-165, 2012.

[12] Y.K. Park and Y. Sung, A reconfigurable antenna for quad-band mobile handset applications, *IEEE Transactions on Antennas and Propagation*, vol. 60, no. 6, pp.3003-3006, 2012.

[13] Z. Zhang, M.F. Iskander, J.C. Langer, and J. Mathews, Dual-band WLAN dipole antenna using an internal matching circuit, *IEEE Transactions on Antennas and Propagation*, vol. 53, no. 5, pp.1813-1818, 2005.

[14] F.G. Zhu, J.D. Xu, and Q. Xu, Reduction of mutual coupling between closely-packed antenna elements using defected ground structure, *Electronics Letters*, vol. 45, no. 12, pp.601-602, 2009.

[15] S.W. Su, C.T. Lee, and F.S. Chang, Printed MIMO-antenna system using neutralization-line technique for wireless USB-dongle applications, *IEEE Transactions on Antennas and Propagation*, vol.60, no. 2, pp.456-463, 2012.

[16] Y. Ou, X. Cai, and K. Qian, Two-element compact antennas decoupled with a simple neutralization Line, *Progress In Electromagnetics Research Letters*, vol. 65, pp.63-68, 2017.

[17] S.D. Assimonis, T.V. Yioultsis, and C.S. Antonopoulos, Computational investigation and design of planar EBG structures for coupling reduction in antenna applications, *IEEE Transactions on Magnetics*, vol. 48, no. 2, pp.771-774, 2012.

[18] K. Payandehjoo, and R. Abhari, Employing EBG structures in multiantenna systems for improving isolation and diversity gain, *IEEE antennas and wireless propagation Letters*, vol. 8, pp.1162-1165, 2009.

[19] Y. Chen, L. Ye, J. Zhuo, Y. Liu, L. Zhang, and M. Zhang, Frequency reconfigurable circular patch antenna with an arc-shaped slot ground controlled by PIN diodes, *International Journal of Antennas and Propagation*, Article ID 7081978, 7 pages, 2017.

[20] P.Y. Qin, Y.J. Guo, A.R. Weily, and C.H. Liang, A pattern reconfigurable U-slot antenna and its applications in MIMO systems, *IEEE transactions on Antennas and Propagation*, vol. 60, no. 2, pp.516-528, 2017.

[21] B. Mun, C. Jung, and M.J. Park, A compact frequency-reconfigurable multiband LTE MIMO antenna for laptop

applications, *IEEE Antennas and Wireless Propagation Letters*, vol. 13, pp.1389-1392, 2014.
[22] S.A. Aghdam, A novel UWB monopole antenna with tunable notched behavior using varactor diode, *IEEE Antennas and Wireless Propagation Letters*, vol.13, pp.1243-1246, 2014.
[23] M.A. El-Tanani and G.M. Rebeiz, High-performance 1.5–2.5-GHz RF-MEMS tunable filters for wireless applications, *IEEE Transactions on Microwave Theory and Techniques*, vol. 58, no. 6, pp.1629-1637, 2010.
[24] Ansys High Frequency Structure Simulator (HFSS); Online] available (Accessed July 2017): www.ansys.com/Products/Electronics/ANSYS-HFSS
[25] T. Taga, Characteristics of space-diversity branch using parallel dipole antennas in mobile radio communications, *Electronics and Communications in Japan (Part I: Communications)*, vol. 76, no. 9, pp.55-66, 1993,
[26] P.N. Fletcher, M. Dean, and A.R. Nix, Mutual coupling in multi-element array antennas and its influence on MIMO channel capacity, *Electronics Letters*, vol. 39, no. 4, pp.342-344, 2003.

Biography of the authors

Vipin Choudhary received the Master of technology degree in wireless communication, electronics from Amity University-UP in 2017 and Licentiate (doctorate) degree in the subject area of Electrical Engineering from KTH Royal Institute of Technology, Stockholm, Sweden, in 2021, respectively. His research interest include on RF and antenna measurements, non-destructive testing, radar measurements, radar imaging, microwave/radar absorbers materials, SAR as well as polarimetry measurements, RF measurement techniques and Signal processing.

Manoj Kumar Meshram received the Ph.D. degree from the Institute of Technology (Banaras Hindu University), Vanarasi, India, in 2001. He joined the Department of Electronics Engineering, Indian Institute of Technology (Banaras Hindu University), Varanasi, India, as a Lecturer, where presently he is working as Professor. His research interests include metamaterials, reconfigurable antennas, UWB antennas, MIMO antennas for handheld devices, Vivaldi antennas, microwave imaging, antennas for WBAN, antennas for airborne systems, frequency selective surfaces, printed microwave passive devices, frequency scanning antenna for radar system, microstrip antenna, ferrites, MMIC, and. He has published 90 papers in national and international journals and conferences. Dr. Meshram is a senior member of IEEE, Member of the Indian Science Congress Association, India, Life Member of Indian Society of Technical Education (ISTE), India, and a Life Member of Institution of Electronics and Telecommunication Engineers (IETE), India. He was the recipient of INSA (Indian National Science Academy) visiting Fellowship 2008–09 from Govt of India to visit South Korea under bilateral exchange program. In 2010, he was awarded with the BOYSCAST (Better Opportunity to Young Scientist in Chosen Area of Science and Technology) fellowship for one year for conducting advance research at McMaster University (Electrical and Computer Engineering), Hamilton, Ontario, Canada, with Prof. Natalia K. Nikolova. He is the recipient of Gandhian Young Technological Innovation (GYTI) Award 2015. He is in the reviewer's list of several reference journals in India and abroad. He is the expert member of the project review committee of the Defence Avionics Research Establishment (DARE), Defence Research and Development Organization (DRDO), India. He has successfully accomplished the transfer of technology under CARS project of Defense Avionics Research Establishment (DARE), DRDO, India. He is managing editor of International Journal of Advances in Microwave Techniques (IJAMT)

Jan Hesselbarth was born in Dresden, Germany, in 1970. He received the Doctorate degree from the Swiss Federal Institute of Technology (ETH Zurich), Switzerland, in 2002. He worked as a design engineer with Huber Suhner, Herisau, Switzerland, from 2001 to 2005, and as a member of technical staff with Bell Labs, Dublin, Ireland, from 2005 to 2008. He then joined ETH Zurich as a senior researcher and lecturer. Since 2011, he has been a professor with the Institute of Radio Frequency Technology, University of Stuttgart, Germany. His research interests are in antennas and millimeter-wave circuits and packaging.

DOI: http://dx.doi.org/10.32452/IJAMT.2022.274282